Interaction of hot electrons with Carbon doped GaN buffer in AlGaN/GaN HEMTs: Correlation with lateral electric field and device failure

Rajarshi Roy Chaudhuri, Vipin Joshi, Sayak Dutta Gupta, and Mayank Shrivastava
Department of Electronic Systems Engineering
Indian Institute of Science (IISc)
Bengaluru, India
e-mail id: mayank@iisc.ac.in

***Abstract*—Device design and technology parameter dependent critical voltage governing interaction of hot electrons with traps in Carbon doped GaN buffer is reported in this work. A mechanism controlling trapping of hot electrons in GaN buffer is proposed corroborating well with the experimental observations. Further, reliability of devices operating beyond critical voltage is analyzed using post failure FESEM and gate leakage analysis.**

Keywords—AlGaN/GaN HEMT; Carbon doped buffer; Hot Carriers, Electroluminescence (EL); Reliability

I. INTRODUCTION

Electroluminescence (EL) emissions from AlGaN/GaN HEMTs have long been used to identify the presence of hot electrons in the device [1]-[3]. EL images are useful indicator of high electric field regions/ hot spots in the device and is an important tool used by device designers to identify failure modes in GaN HEMTs and to address hot electron triggered reliability issue [4]-[6]. However, EL spectrum of AlGaN/GaN HEMTs and its dependence on device design and technology parameters is not well understood. In this work, we report use of EL spectrum in identifying the critical drain stress voltage required for interaction of channel electrons with acceptor traps in GaN buffer and its dependence on lateral device parameters. Based on the EL studies, the mechanism behind ionization of acceptor traps in C-doped GaN buffer is proposed which corroborates well with experimentally observed critical voltage for interaction of hot electrons with buffer traps. Finally, post failure SEM analysis is done to correlate interaction of hot electrons with buffer traps and device failure.

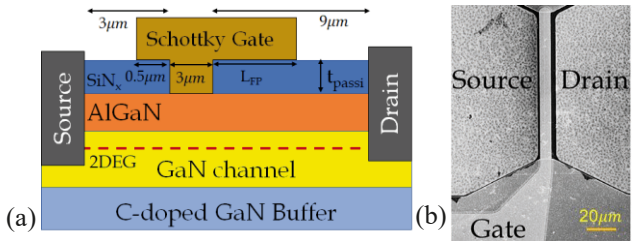

Fig. 1: (a) Device schematic of fabricated Schottky gated AlGaN/GaN HEMT on 600-V commercial grade GaN-on-Si epi-stack, (b) FESEM image of the top view of the device indicating the source, drain and gate contacts.

II. DEVICE DESIGN AND EXPERIMENTAL SETUP

The EL studies were carried out on AlGaN/GaN HEMT devices fabricated on a 600-V commercial grade GaN stack for power applications shown in Fig. 1. Measurements were done using Horiba micro-Raman spectroscopy setup. A confocal microscope was used to collect the EL signals emanating from the device biased in semi-ON condition ($V_{GS} \approx V_{Th}+1V$). The signals were collected from a well-defined spot of size ~1 μm to obtain the spectral information over a wavelength range of 350 nm to 850 nm.

III. INTERACTION OF HOT ELECTRONS WITH BUFFER TRAPS

Fig. 2a depicts EL spectrum at the drain edge (DE) of the device extracted for different drain voltages ($V_{DS\text{-}Stress}$). For lower $V_{DS\text{-}Stress}$, the EL signal has a long Maxwellian tail-like feature. With an increase in $V_{DS\text{-}Stress}$, EL signals show two distinct trends- (1) it covers wide energy range, and

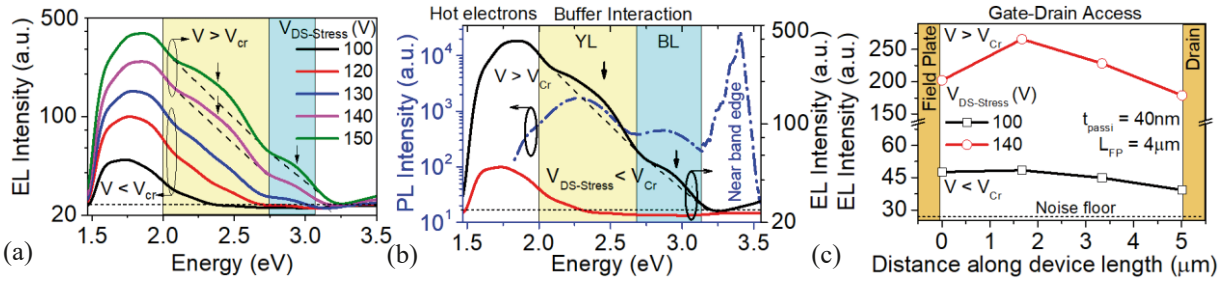

Fig. 2: (a) EL spectra of a device extracted at drain pad edge indicates a critical voltage ($V_{Cr} \approx 140$ V) beyond which defect related signals manifest in the EL spectra. Arrows indicate defect-related signals manifesting as deviations from Maxwellian tail (shown as dotted line), (b) Comparative study of PL and EL spectra shows yellow (YL) and blue luminescence (BL) bands for $V_{DS\text{-}Stress} > V_{Cr}$, (c) EL line scan shows uniform intensity distribution between drain and gate field plate for $V_{DS\text{-}Stress} > V_{Cr}$ as well as $V_{DS\text{-}Stress} < V_{Cr}$. Device dimensions are $L_{FP} = 4$ μm & $t_{passi} = 40$ nm.

This work was financially supported by Department of Science and Technology (DST), Govt. of India, under project grant no. DST/TSG/AMT/2015/294.

978-1-7281-4836-6/20/$31.00 ©2020 IEEE

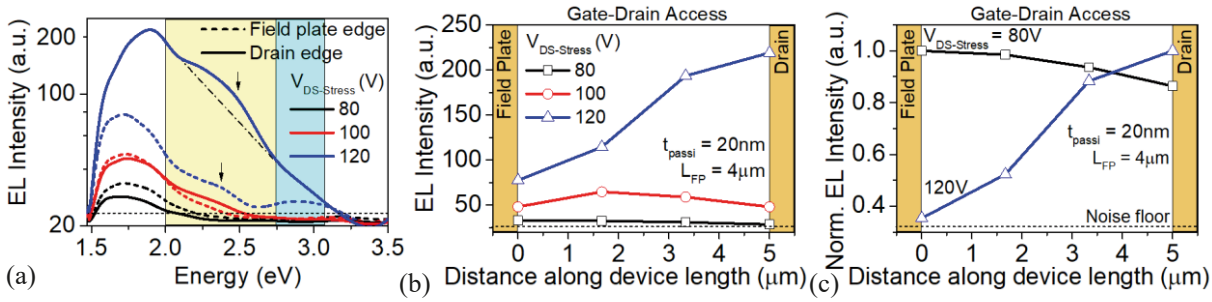

Fig. 3: (a) EL spectra at drain edge for a device with thinner passivation shows a critical voltage (~120V) which is lower than that observed for the device with thicker passivation (~140V). Negligible buffer defect signal is observed at the field plate edge. (b) EL line scan &, (c) Normalized EL line scan for the device depicts a non-uniform profile with a shift in EL intensity peak from field plate edge to drain edge as $V_{DS-Stress}$ is increased beyond V_{Cr}, indicating an extension of depletion region up to the drain edge accompanied by an increase in EL intensity.

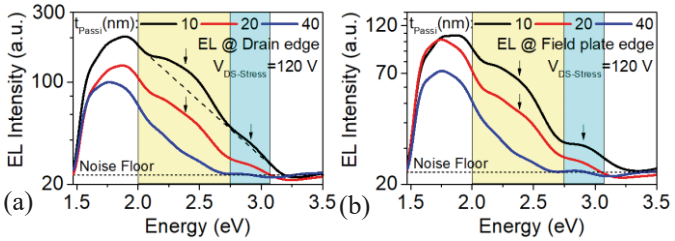

Fig. 4: EL spectrum extracted at (a) Drain edge, and (b) Field plate edge for devices with different passivation thickness. With reduction in passivation thickness, an increase in EL intensity is seen with buffer defect signal appearing at both the edges for sufficiently thinner passivation. Device dimensions are L_{GD} = 9µm & L_{FP} = 4µm.

(2) appearance of prominent signals with distinct peak in the energy ranges of ~2 eV-2.7 eV (Yellow luminescence) and ~2.7 eV- 3.2 eV (Blue luminescence) which overlap with the buffer related defect/trap transitions (Fig. 2b), signifying interaction of hot electrons with traps in GaN buffer. Further, Fig. 2a highlights a critical $V_{DS-Stress}$ (V_{Cr}) beyond which hot electrons interact with buffer traps. EL line scans along the access region (Fig. 2c) depict uniform distribution of EL intensity above and below V_{Cr} indicating channel depletion up to the DE. V_{Cr} is then defined by the threshold energy/concentration of hot electrons required for interaction with buffer traps. EL line scans for a device with thinner SiN passivation depicts a non-uniform EL distribution with shift in EL peak from field plate edge (FPE) to DE (Figs. 3b & 3c) as $V_{DS-Stress}$ is increased beyond V_{Cr}, indicating extension of depletion region up to the DE for $V_{DS-Stress} > V_{Cr}$ (Fig. 3a). V_{Cr} is thus defined by the voltage required for depletion region to extend up to the DE in addition to the threshold EL intensity required for interaction of hot electrons with buffer traps. EL spectrum for devices with different passivation thickness (t_{passi}) depicts that devices with thinner passivation exhibit increased buffer defect signal intensity at the DE (Fig. 4a) with buffer defect signal now appearing even at the FPE (Fig. 4b).

IV. Mechanisms Governing Buffer Trap Ionization by Hot Electrons

Figs. 5 (a)-(d) depicts the mechanism governing interaction of hot electrons with buffer traps. Presence of a threshold energy for interaction of hot electrons with buffer traps is explained by considering negatively charged layer present near the GaN channel due to ionization of acceptor traps in C-doped region. The resulting electric field ($E_{vertical}$) prevents further trapping of channel electrons in the buffer traps (Fig. 5a) under thermal equilibrium. An extension of depletion region up to DE enable highly energized hot electrons near DE to overcome $E_{vertical}$ and interact with buffer traps, emitting buffer defect signal (Fig. 5b, Figs. 3a & 3c). Further, hot electrons under the FPE in devices with higher t_{passi} do not gain sufficient energy to overcome $E_{vertical}$ while those in devices with lower t_{passi} gain sufficient energy to overcome $E_{vertical}$ and interact with buffer traps due to lateral and vertical extension of depletion region (Figs. 5c, 5d & 4b). Fig. 6 depicts an increase in V_{Cr} as field plate length is reduced or as t_{passi} is increased, which is in

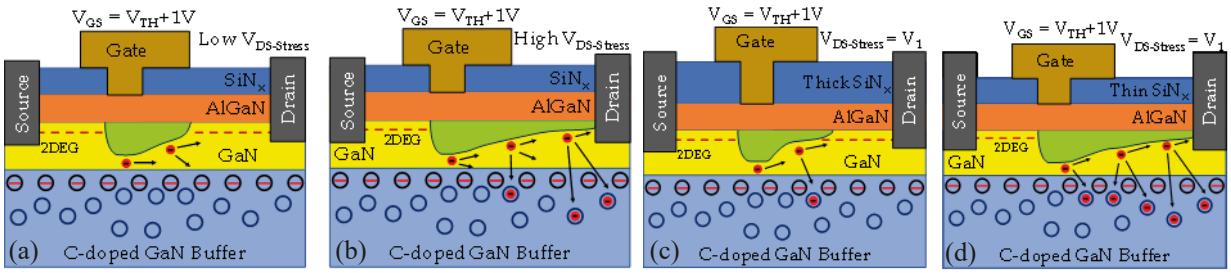

Fig. 5: Schematic depicting proposed mechanism for interaction of hot electrons with buffer traps. (a) Condition where depletion region is confined near gate/field plate edge and is not able to provide sufficient energy to hot electrons to cross-over the vertical barrier due to presence of ionized acceptor traps in C-doped GaN buffer, (b) condition in which depletion region extends up to the drain edge giving sufficient energy to hot electrons near the drain edge to cross-over the vertical barrier and interact with traps in deeper GaN buffer, (c) condition where presence of a thicker passivation layer doesn't allow the depletion region to extend laterally as well as vertically for electrons to gain sufficient energy to cross-over the vertical barrier, and (d) condition where reduction in passivation thickness extends depletion region laterally as well as vertically beneath the field plate enabling capture of hot electrons in the deeper GaN buffer enabling buffer trap related EL transitions.

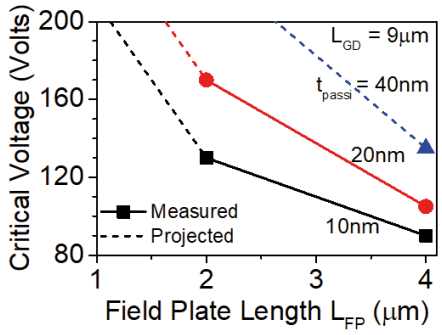

Fig. 6: Critical voltage as a function of device design parameters depicting a higher critical voltage for devices with thicker passivation and shorter field plate. Dotted line shows the projected values as the critical voltage for these devices was not observed up to the measurement range of 200 V.

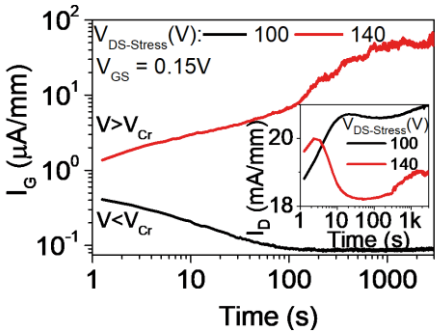

Fig. 7: Gate current transients reveal a drastic increase in gate current as stress voltage is increased beyond V_{Cr}. This indicates device degradation as hot electrons begin interaction with buffer traps. Inset shows the transient evolution of drain current during semi-ON state stress.

agreement with the above proposed mechanism.

V. Impact on Device Reliability

Fig. 7 depicts a drastic increase in gate leakage for $V_{DS-Stress} > V_{Cr}$ which is an indicator of gate degradation. Fig. 8a indicates the presence of multiple cracks and pits (shown in Fig. 8b) with localized failure in the gate-drain region. However, the failure spot is rather moderate and extended in the source pad. Such localized failure and formation of cracks & pits in the gate-drain access region, visible in FESEM images of the failed devices (Fig. 8a & 8b), suggest hot electron induced failure. In order to investigate the effect of passivation thickness on the nature and extent of device failure, FESEM images for a device with higher passivation thickness (t_{Passi}= 40 nm) were analyzed. Fig. 8c shows the extent of failure in one such device. It can be seen that, the density of cracks and pits are lower for devices with thicker passivation, than that for devices with lower t_{Passi}. Further, Fig. 8d shows the pits and cracks in the gate-drain region for a device having higher t_{Passi}. A moderate device failure observed for devices with higher t_{passi} as compared to devices with lower t_{passi}, which justifies the role of buffer interacting hot electrons in device failure. It is imperative to highlight here that the devices that failed during EL study had hot electrons interacting with the buffer traps as seen from their EL spectra.

VI. Conclusion

With this work we have shown that EL spectrum of AlGaN/GaN HEMTs exhibits typical defect peaks particular to the buffer trap signals beyond a critical drain voltage. The critical drain voltage was found to be dependent on (i) EL intensity near the drain edge, (ii) lateral extent of depletion region and (iii) vertical extent of depletion region beneath the field plate. Device design and technology parameters were found to affect the critical voltage, suggesting device design for improved device reliability in presence of hot electrons. Gate leakage was found to increase drastically post critical stress voltage. Further, post failure device analysis revealed a hot electron driven failure with formation of cracks and pits in devices where buffer defect signal was prominent in the EL spectrum.

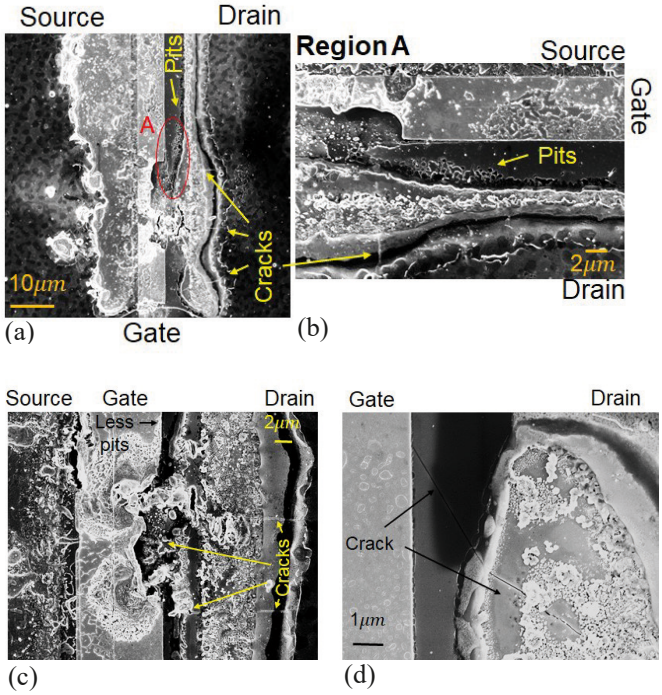

Fig. 8: FESEM of devices that failed during EL study: (a) Device with t_{passi} = 20nm shows catastrophic failure in the gate finger and drain pads. (b) Magnified view of the region A (marked in red circle in Fig. 8a) (c) Failure in HEMTs with t_{passi} = 40nm is moderate with lower density of cracks and pits. (d) Reduced pit and crack density in the failure spot at the gate-drain access region for thicker t_{passi}

Acknowledgment

This work was funded by Department of Science and Technology (DST), Govt. of India, under project grant no. DST/TSG/AMT/2015/294. Authors would like to acknowledge people at National Nanofabrication Centre (NNfC), Micro Nano Characterization Facility (MNCF) and the GaN group in Indian Institute of Science, Bangalore for their help and fruitful discussions. Student authors Rajarshi Roy Chaudhuri and Sayak Dutta Gupta would like to thank DST INSPIRE for their fellowship.

REFERENCES

[1] N. Shigekawa, K. Shiojima and T. Suemitsu, "Electroluminescence characterization of AlGaN/GaN high-electron-mobility transistors", Applied Physics Letters, vol. 79, no. 8, pp. 1196-1198, 2001. DOI: 10.1063/1.1398332.

[2] T. Brazzini, H. Sun, F. Sarti, J. W. Pomeroy, C. Hodges, M. Gurioli, A. Vinattieri, M. J. Uren and M. Kuball, "Mechanism of hot electron electroluminescence in GaN-based transistors", Journal of Physics D: Applied Physics, vol. 49, no. 43, p. 435101, 2016. DOI: 10.1088/0022-3727/49/43/435101.

[3] M. Meneghini, N. Ronchi, A. Stocco, G. Meneghesso, U. K. Mishra, Y. Pei and E. Zanoni, "Investigation of Trapping and Hot-Electron Effects in GaN HEMTs by Means of a Combined Electrooptical Method," in *IEEE Transactions on Electron Devices*, vol. 58, no. 9, pp. 2996-3003, Sept. 2011. DOI: 10.1109/TED.2011.2160547

[4] C. Hodges, N. Killat, S. W. Kaun, M. H. Wong, F. Gao, T. Palacios, U. K. Mishra, J. S. Speck, D. Wolverson and M. Kuball., "Optical investigation of degradation mechanisms in AlGaN/GaN high electron mobility transistors: Generation of non-radiative recombination centers", Applied Physics Letters, vol. 100, no. 11, p. 112106, 2012. DOI: 10.1063/1.3693427

[5] I. Rossetto, M. Meneghini, A. Tajalli, S. Dalcanale, C. D. Santi, P. Moens, A. Banerjee, E. Zanoni, G. Meneghesso, "Evidence of Hot-Electron Effects During Hard Switching of AlGaN/GaN HEMTs," in *IEEE Transactions on Electron Devices*, vol. 64, no. 9, pp. 3734-3739, Sept. 2017. DOI: 10.1109/TED.2017.2728785.

[6] F. Gütle, V. M. Polyakov, M. Baeumler, F. Benkhelifa, S. Müller, M. Dammann, M. Cäsar, R. Quay, M. Mikulla, J. Wagner and O. Ambacher, "Radiative inter-valley transitions as a dominant emission mechanism in AlGaN/GaN high electron mobility transistors", *Semiconductor Science and Technology*, vol. 27, no. 12, p. 125003, 2012. DOI: 10.1088/0268-1242/27/12/125003.